

Application of robotic technologies for the fabrication of traditional Chinese timber joints

Jiangyang Zhao¹, Davide Lombardi², Agkathidis Asterios³

^{1,3}University of Liverpool, Architecture School ²Xi'an Jiaotong - Liverpool University, Department of Architecture

^{1,3}{psjzha32|a3lab}@liverpool.ac.uk ²Davide.Lombardi@xjtlu.edu.cn

The Design of traditional Chinese buildings was influenced by the climate and the sociogeographical conditions of the different regions in China. They were usually constructed out of wood (Liang, 2005) relying on timber-joint based construction systems. Amongst the wide variety of the structural elements, the Dougong bucket arch is one of the most common components of traditional wooden framework buildings, presenting a high level of complexity (Liang, 2005). Parametric design and robotic technology enable new possibilities regarding its fabrication and application in contemporary architecture. Our paper will explore how the Dougong bucket arch joint components could be reinvented through the use of parametric tools and robotic fabrication methods and thus applied in contemporary architectural structures. Our findings will provide an insight into the traditional construction principles of the joint and how these can inform a design and fabrication framework for its application in contemporary buildings.

Keywords: *Dougong joint, timber structures, parametric design, robotic fabrication, optimization*

INTRODUCTION

A brief history of the Dougong joint

The Dougong bucket arch is an independent category, withing the traditional Chinese timber framework systems. It consists of many different types of Dou (square load-bearing member) and Gong (arch load-bearing member), (Liang, 2005). During the Qing dynasty, there were even specialised Dougong making craftsmen, called Dougong carpenters (Dehua, 2011).

Historically, the main structure of traditional Chinese buildings is a load-bearing timber framework while the walls are part of the building. The roof's

structural load is transferred from the beam purlin to the pillar into the structural system. There is a complex component named Dougong, which is a transition component between the beam purlin and the pillar. It has been a unique element of Chinese architecture for thousands of years. (Liang, 1985)

The earliest Dou appeared during the bronze age of the Shang and Zhou Dynasties, and the appearance of Gong followed later (Dehua, 2011). According to Yang Hongxun's 'Architectural Archaeology Study of Tomb Buildings, Murals and Burial Artefacts, the structure of Dougong had been widely used and achieved its mature stage since the Han dynasty, 206

BC-220 AD, (Dunzhen, 1982).

The proportions and the name of the Dougong components before the Song Dynasty (960-1279) are difficult to retrieve since there are not related sources to refer to. However, two important historic rulebooks the Yin Zhao Fa Shi and the Gongchen Zuofa Zeli provide both standards and structural regulations for buildings and building components. The first was completed by Li Jie in the Song Dynasty (960-1279) while the second was published by the Ministry of Construction of the Qing Dynasty in 1734. In this paper, we mainly focus on studying the Dougong developed during the Qing dynasty (1636-1911) as a large number of buildings from this period have been preserved and can provide a reliable database for analysis.

Dougong types

The size, the structure, the technology and the materials of at least thirty different Dougong joints are recorded in the historic rulebook Gongchen Zuofa Zeli. They can be classified based on their function and position inside the building (Ma, 2003). A first classification can be obtained by dividing the Dougong into two main categories according to its position: a Dougong located in the extension of the building is called 'the external eave Dougong' and the one located inside the eaves is called 'the inner eave Dougong'. Furthermore, the external eave Dougong can be divided into an intermediate set, a column set and corner set (Ma, 2003). This paper will mainly focus on the external eave Dougong, and particularly the intermediate set (Figure 1).



Dougong components

The Dougong balances the weight of the roof and transfers its loads from the roof to the pillars. Traditionally it was built manually, requiring a significant amount of time for its completion. It is composed of five different components (Figure 2), which include: the Gong, Qiao, Ang, Dou, and Sheng, (Liang 2006).



Figure 2
Components' of the
Dougong

In modern years the ancient knowledge and applications of the Dougong are disappearing. We are confident that parametric design tools and robotic fabrication techniques could be used for the reinvention of the joint and ensure its survival into the modern era. In particular, our research will try to answer the following questions:

1. How can we simplify the Dougong elements by using parametric modelling tools and robotic fabrication techniques?
2. How could a reinvented joint be applied in contemporary architecture?

To achieve this we will start by studying different cases studies which have applied robotic technology to reproduce wooden joints. We will then propose a framework which will integrate the traditional construction and design principles embedded in the Dougong and will allow us to reinvent the ancient joint.

Figure 1
Principal parts of a
Chinese
timber-frame
building. (Drawn by
the 'Society for
Research in Chinese
Architecture')

RESEARCH CONTEXT AND LITERATURE

Digitalisation and robotic reproduction of elements of a Japanese traditional timber system are being described by Takabayashi et al. (2018). In their experiment, the Japanese team introduced a novel method for the robotic reproducing a roof corner detail of a Japanese pagoda by using five tools; a circular saw, a square chisel, a vibration chisel, a router and a five axes KUKA KR 6R 700 robotic arm to reproduce the different joint components. The robotic toolpath was generated by a specifically developed CAM programme. As Japanese timber systems are based on Chinese systems, this method provides valuable insights into designing and creating Chinese joints too. However, this study does not attempt to reinvent the traditional elements, neither examines their application on modern-day design driven by robotic technology and parametric design tools.

The research team led by Heesterman and Sweet (2018) investigated the use of parametric tools and robotic technology to reproduce traditional joints, suitable for contemporary architectural applications. They employed a 6-axis ABB IRB 6700 robotic arm and the HAL Grasshopper plug-in, to produce a set of physical prototypes using mortise splices and curved splices in their attempt to explore possible new joints. As a starting point, the researchers fabricated a simple physical model by using a CNC mill to identify possible deficiencies. The data from that first experiment helped them to identify and resolve issues before proceeding with the robotic fabrication.

The research team led by Böhme explored the potential of applying robotic fabrication for the reconstruct a historical joint employing parametric tools and a KUKA KR125/2 and Agilus KR6 R900 Sixx robotic arms. The experiment's findings suggested that the process can be successful without modifying the joint's geometry.

The team led by Yuan Feng explored how to use a 5 axis CNC router to design and fabricate a structural installation based on a traditional Chinese eaves rafter. Firstly, they analyzed the bending moments of the joint by using the Grasshopper plugin Milli-

pede. After finding out about the underlying structural principles, they designed an umbrella-shaped structural installation by using a unit based on the traditional rafter proportions. In the structural simulation stage, the topology function was applied to optimize the dimensions of the unit before proceeding with its robotic fabrication.

Chai and Yuan, (2018) fabricated a complex wooden pavilion at the University of Tongji, using a gantry robotic system and the Grasshopper plugin Karamba3D, as well as a KUKA R2700 robotic arm. They developed a band-saw end-effector and applied it to fabricate curved wooden beams and mortise-tenon joints. The experiment proves that robotic arms can fabricate complex wooden structures with their band-saw end-effector more efficiently and accurately than with a CNC mill.

Finally, in a case study conducted at the University of Sydney (Page, 2017), Dove, an open-source software plugin was used for developing a 3D model of a timber joint. The physical prototype was fabricated by a KUKA KR60 6-axis robot and a milling spindle end-effector. They have also developed a tool, which is reducing milling time, simplifying the tool paths and saves material.

All the projects presented here are investigating how to reproduce building components or building parts by employing robotic technology based on the proportions of the original structure. In contrast, our work will focus on how we could re-invent the Dougong joint, thus to apply it in contemporary design solutions.

METHODOLOGY

Our research method consists of a design experiment and its validation via digital simulation and physical prototyping. In particular, our method includes four main phases and a feedback loop.

In phase one we will analyse the Dougong's components and proportions, based on sources referring to the Qing dynasty, where the Doukou system (bucket mouth system) is used as a standard unit for each building module. This system is an optimised

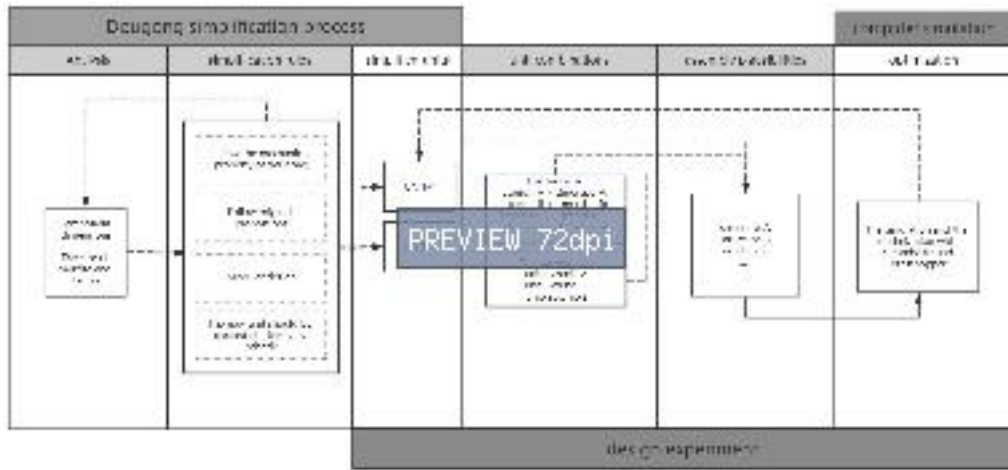


Figure 3
Research
methodology
framework

version of the Caifen system, which was developed during the Song in dynasty.

In the second phase, we will simplify the joint and develop a digital, parametric modelling framework of a novel design unit, with references to the proportions and the structural properties of the traditional Dougong as well further geometrical properties allowing it to be robotically fabricated.

Phase three includes the structural simulation and optimisation of the design unit. We will test both a linear and a non-linear structure using the Karamba3D plug-in for Grasshopper. Phase three will also include a robotic fabrication simulation using the firmware RoboDK and Grasshopper. A feedback loop to face two is included here, making sure that all simulation results will feed back into the original design starting point. Finally, in phase four, which will not be included in this paper, we will proceed to the validation of or design framework via a physical prototype using a CNC mill and UR 10 robotic arm. The CNC milled prototype will help us to optimise the fabrication process, prior to its final fabrication destination, the UR10 robotic arm. That will also include the development of the appropriate end-effectors. This paper will cover the analysis of proportions and

mechanical properties of the Dougong, the reinvention of its unit, the assembly possibilities of the new units, and their simulation and optimization of in Karamba3D (Figure 3).

DESIGN EXPERIMENT

As previously described, our design experiment consists of the analysis of the traditional Dougong proportions and design rules, as well as the parametrisation of a novel design unit. Firstly, we will study Dougong's proportions by reviewing the two rule books mentioned previously. We will then design the unit according to the mechanical properties as described by Yuan (2012), using the proportions and connection methods as recorded in the books Qishi Yin Zhao Zeli (Liang, 2006) and Gong Chen Zuo Fa (Liang, 2006) and the Chinese ancient architecture woodwork construction technology manual (Ma, Bingjian. 2003). In parallel, other parameters contributing to the efficient robotic fabrication of the unit and its clusters will be applied.

Analysis

There are eleven classes in the Doukou system . The width of the first-class Dou is 19.2cm, thus the width

Figure 4
simplified structure
model of Dougong
(Yuan, 2012)

Table 2
rules of unit 1 and
unit 2

Figure 5
the parametric
models for unit 1
and unit 2

of one Doukou is 19.2cm. Each class is linked to a particular building function and any change from class to class is based on the formula:

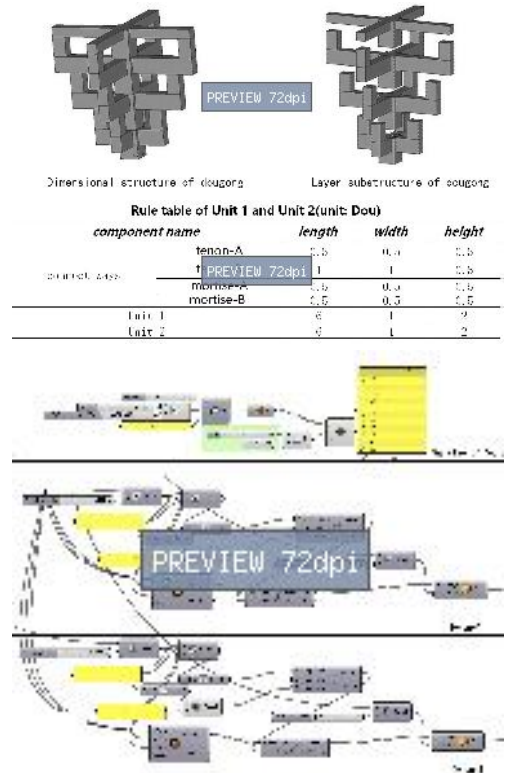
$1 \text{ Dou} = 19.2\text{cm} + (11 - N) * 0.5 \text{ Cun}$,
(1Cun=3.33cm), N: the class of Cai (1, 2, 3, 4, ..., 11);
Cun is the traditional unit of length in China.

We will use the table and the formula to design all components for our design experiment. The intermediate set will be explored firstly, as described by Ma (2003) in table 1. The distance of the main stress points is 3 Dou according to the proportion analysis of the Dougong components (Table 1). The connection method of the components is based on the principle of mortise and tenon. A tenon is usually located between two stress points. Two stress points are connected with a mortise. One Dougong element is composed of at least one tenon and two mortises.

Parametric design framework of novel design unit

The new unit should respect the proportions and the structural properties of the traditional Dougong allowing the unit to be fabricated by a robotic arm. A way to do that is by minimizing it to the way the components are being connected as well as its mechanical properties as demonstrated in figure 4, (Yuan et al. 2012). We have chosen the second layer of an interlocked bracket set including the first transverse bracket arm (X) and the axial oval arm (X) as shown in Table 1. The length, the width and the height of the two elements are adjusted to integers, the decorative elements and the complex curve can be removed aiming to improve the effectiveness of its robotic fabrication (Table 2).

We have parametrized the two main Dougong units using Grasshopper (Figure 6). The units are composed of four elements: tenon A, tenon B, mortise A and mortise B (Figure 5).



There are three main rules of connection possibilities (Table 4): unit 1 & unit 2, unit 1 & unit 1 and unit 2 & unit 2. Furthermore, every connection type includes three different unit groups: the square-shape (P 1, P 2, and P 3), the T-shape (P 1-1, P 2-1, and P 3-1), the cross-shape (P 1-2, P 2-2, P 3-2) and L-shape (P 1-3, P 2-3, and P 3-3) respectively, which is the basic shape of the assembly (Figure-7). According to these rules, the combination of different units will produce different results of assembly. In our paper, we are assessing seven design units, A, B, C, D, E, F and G (Figure-8). The key element of structure A is P-1-2 (possibility-1-3), and the key elements of structure B are P-1, P-1-2, and P-3-3. The connection method of the two structures is P-2-2 and P-3-2. P-1-1 is applied in structure C as the key element. Structure D consists

Component	Length	Width	Height
Unit 1 (P-1)	1	1	1
Unit 2 (P-2)	1	1	1
Unit 3 (P-3)	1	1	1
Unit 4 (P-4)	1	1	1
Unit 5 (P-5)	1	1	1
Unit 6 (P-6)	1	1	1
Unit 7 (P-7)	1	1	1
Unit 8 (P-8)	1	1	1
Unit 9 (P-9)	1	1	1
Unit 10 (P-10)	1	1	1
Unit 11 (P-11)	1	1	1
Unit 12 (P-12)	1	1	1
Unit 13 (P-13)	1	1	1
Unit 14 (P-14)	1	1	1
Unit 15 (P-15)	1	1	1
Unit 16 (P-16)	1	1	1
Unit 17 (P-17)	1	1	1
Unit 18 (P-18)	1	1	1
Unit 19 (P-19)	1	1	1
Unit 20 (P-20)	1	1	1
Unit 21 (P-21)	1	1	1
Unit 22 (P-22)	1	1	1
Unit 23 (P-23)	1	1	1
Unit 24 (P-24)	1	1	1
Unit 25 (P-25)	1	1	1
Unit 26 (P-26)	1	1	1
Unit 27 (P-27)	1	1	1
Unit 28 (P-28)	1	1	1
Unit 29 (P-29)	1	1	1
Unit 30 (P-30)	1	1	1
Unit 31 (P-31)	1	1	1
Unit 32 (P-32)	1	1	1
Unit 33 (P-33)	1	1	1
Unit 34 (P-34)	1	1	1
Unit 35 (P-35)	1	1	1
Unit 36 (P-36)	1	1	1
Unit 37 (P-37)	1	1	1
Unit 38 (P-38)	1	1	1
Unit 39 (P-39)	1	1	1
Unit 40 (P-40)	1	1	1
Unit 41 (P-41)	1	1	1
Unit 42 (P-42)	1	1	1
Unit 43 (P-43)	1	1	1
Unit 44 (P-44)	1	1	1
Unit 45 (P-45)	1	1	1
Unit 46 (P-46)	1	1	1
Unit 47 (P-47)	1	1	1
Unit 48 (P-48)	1	1	1
Unit 49 (P-49)	1	1	1
Unit 50 (P-50)	1	1	1

Table 1
Rules and proportions of the intermediate set



Figure 6
names of tenon and mortise for Unit-1 (left) and Unit-2(right)

Unit	2tenon-A + 2mortise-A	2mortise-B + 1mortise-B	1tenon-A + 2mortise-A	1tenon-B + 2 mortise -B
unit 1 & unit 2	1-1 (joint 1-1)	-	1-2 (joint 1-2)	1-1 (joint 1-1)
unit 1 & unit 1	1-2 (joint 1-2)	-	1-1 (joint 1-1)	1-2 (joint 1-2)
unit 2 & unit 2	1-1 (joint 1-1)	1-2 (joint 1-2)	1-2 (joint 1-2)	1-1 (joint 1-1)

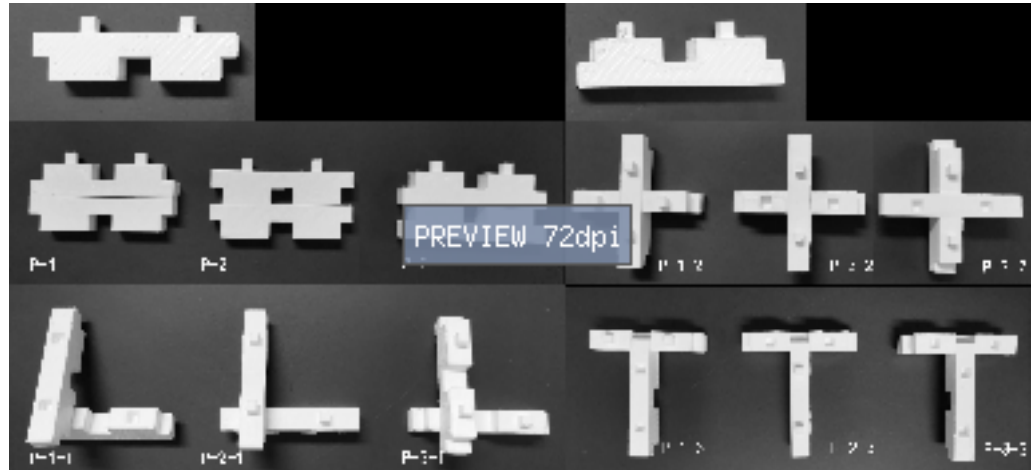
Table 3
The rule of assembly

of the P-3-3 unit, the structure E consists of the P-3, P-2 and P-1-2 units, and the structures F and G consist of the P-1-2 unit.

The structure was developed by two basic rules: Rule one is based on the combinations of unit 1 & unit 2, unit 1 & unit 1 and unit 2 & unit 2. Rule two is based on the combinations of 2 tenon A + 2 mor-

tise A; 1 tenon B + 1 mortise B; 1 mortise B + 1 mortise B; 1 tenon A + 1 mortise A. The & symbol indicates the combination of two units. For example, unit 1 & unit 2 means one element consists of unit 1 and unit 2. The '+' symbol indicates the connection method of two units. For example, 2 tenon A + 2 mortise A means that the two tenon A of one unit connects with the

Figure 7
The rule of
assembly



two mortise A of another one unit.

SIMULATION AND OPTIMIZATION

According to the mechanical performance of the units in the structural system simulation, this part of the research is mainly to optimize its cross-section employing a genetic algorithm by using the Galapagos and the Karamba plugins for Grasshopper. We choose to perform the optimization on structure G, as it is the most complex. Our unit is built based on the first Cai level, equal to one Dou=19.2 cm. Therefore, the width, height, and length of two units is 1 Dou (19.2 cm), 1.4 Dou (26.88cm) and 6 Dou (115.2cm). According to, Yuan (2012), the unit can be simplified to a rectangular box for its mechanical analysis in the simulation software. We have assumed that the structure could be applied as a support structure of a dwelling, thus the load applicable for this case would be 3.0 kN/m² according to the data of the table A.2.3.2 provided by Karamba [1].

The uniform load of one unit is 0.8232kN/m approximately equal to 1 kNm as calculated by the formula $q=b*q'$, where q stands for the uniform line load, b for the beam width and q' for the uniformly distributed load. Therefore, we have applied

the uniform load 1kN/m for our Karamb3D simulation (Figure-9). The elastic energy of structure G is 0.001334kNm according to Karamba3D. Based on these inputs, the optimal cross-section dimensions are 0.5dou*0.5dou. According to table 2, the Dougong width is between 1 Dou and 1.24 Dou, and its height is between 1.4 Dou and 2 Dou, which is the Dougong rule. This result does not follow the Dougong rule.

The uniform load of one unit is 0.8232kN/m approximately equal to 1 kNm as calculated by the formula $q=b*q'$, where q stands for the uniform line load, b for the beam width and q' for the uniformly distributed load. Therefore, we have applied the uniform load 1kN/m for our Karamb3D simulation (Figure-9). The elastic energy of structure G is 0.001334kNm according to Karamba3D. Based on these inputs, the optimal cross-section dimensions are 0.5dou*0.5dou. According to table 1, the Dougong width of the cross-section should be between 1 Dou and 1.24 Dou, and its height should be between 1.4 Dou and 2 Dou. The data suggested by the experiment is out of the specified restrict of the dimension of the cross-section.

Within this data set, we will proceed with the cal-



Figure 8: The different assembly possibilities



Figure 9: The different assembly possibilities



Figure 10: The different assembly possibilities

Figure 8
The different
assembly
possibilities

culatation the optimal length and width of the section employing the Galapagos plugin (Figure-9). The re-

sult shows that the elastic energy being closest to 0.00937 kNm is 0.001321kNm. At the same time, the dimensions of the crass section are 1.5 Dou

(29.4cm)high and 1.1 Dou (21.56cm)wide following the rule of the Dougong.

Figure 9
the result of
simulation in
Karamba3D



DISCUSSION AND CONCLUSION

The paper explored a strategy for simplifying the elements of Dougong to make it more suitable for contemporary architectural applications. According to the mechanical properties and proportions of the Dougong, we simplified two elements of the interlocking bracket set via adjusting its dimensions to the integers and removing the decorative elements and the complex curves. Furthermore, we designed two units and defined two rules of connecting the units based on the connection way of the Dougong. The inter-combination of the unit will form different assembly possibilities following the described rules. We have explored seven assembly possibilities and simulated one of them in Karamba3D. The dimensions of the unit were optimized to be 1.1 Dou in width and 1.5 Dou in height.

The analysis of the results concluded to the following outcomes: firstly, when the dimension of the cross-section is 1.5 Dou in height and 1.1 Dou in width, the elastic energy of the structure is 0.001321kNm according to the optimization outcome. However, before the optimization, the energy of the structure was 0.001334kNm only 0.000013kNm higher to the original cross-section, which proves that the original structure, was optimized empirically for centuries, despite the lack of high-tech tools. Simplified and optimized joints have the potential to be integrated into contemporary design solutions.

However, as we currently only focused on the intermediate Dougong set, we will continue applying this method to design a new unit based on the study of the column and corner sets and finally develop a data table to facilitate the robotic fabrication of the timber unit. We will also explore the applicability of our unit on modern designs, such as the structures of a bridge and a pavilion.

IMAGE CREDITS

Figure 4: Yuan, JL, Shi, Y, Chen, W and Wang, J 2012, 'Finite element model of Dou-Gong based on energy dissipation by friction-shear', *Journal of Building Structures*, 06, p. 33.

REFERENCES

- Böhme, LFG, Zapata, FQ and Ansaldo, SM 2017, 'Roboticus tignarius: robotic reproduction of traditional timber joints for the reconstruction of the architectural heritage of Valparaiso', *Construction Robotics*, 1, pp. 61-68
- Hua, C and Yuan, F 2018, 'Investigations on Potentials of Robotic Band-Saw Cutting in Complex Wood Structures', in Willmann, J, Block, P, Hutter, M, Byrne, K and Schork, T (eds) 2018, *Robotic Fabrication in Architecture, Art and Design*, Springer Cham, pp. 256-269
- Liang, S 1985, *Anthology of Liang Sicheng*, China Construction Industry Press
- Liang, S 2005, *Chinese architecture: a pictorial history*, Dover Publications
- Liang, S 2006, *Qing "Gong Chen Zuo Fa" graphic*, Tsinghua University Press
- Liu, DZ 1982, *Anthology of Dunzhen Liu*, China Construction Industry Press
- Ma, BJ 2003, *Chinese ancient architecture woodwork construction technology*, Science Press
- Mikayla, H and Kevin, S 2018 'Robotic Connections: Customisable Joints for Timber Construction', *Proceedings of the 22nd Conference of the Iberoamerican Society of Digital Graphics*, pp. 644-652
- Mitchell, P 2017 'A Robotic Fabrication Methodology for Dovetail and Finger Jointing: An Accessible & Bespoke Digital Fabrication Process for Robotically-Milled Dovetail & Finger Joints', *Proceedings of ACADIA*, pp. 456- 463
- Pan, DH 2011, *Dougong*, Southeast university Press, Nanjing



Figure 10
optimization
algorithm using
Karamba3D

Takabayashi, H, Kado, K and Hirasawa, G 2018, 'Versatile Robotic Wood Processing Based on Analysis of Parts Processing of Japanese Traditional Wooden Buildings', in Willmann, J, Block, P, Byrne, K and Schork, T (eds) 2018, *Robotic Fabrication in Architecture, Art and Design*, Springer, Cham, pp. 221-231

Yuan, P.F and Chai, H 2019, 'Reinterpretation of Traditional Wood Structures with Digital Design and Fabrication Technologies', in Bianconi, F and Filippucci, M (eds) 2019, *Digital Wood Design*, Springer, Cham

Yuan, J.L, Shi, Y, Chen, W and Wang, J 2012, 'Finite element model of Dou-Gong based on energy dissipation by friction-shear', *Journal of Building Structures*, 06, p. 33

[1] <https://manual.karamba3d.com/appendix/a.4-background-information/a.4.3-tips-for-designing-statically-feasible-structures#table-a-2-3-2-loads-for-typical-scenarios>